Transcriptional regulation of photosynthesis under heat stress in poplar

Yiyang Zhao
Beijing Forestry University
Jianbo Xie
Beijing Forestry University
Weijie Xu
Beijing Forestry University
Sisi Chen
Beijing Forestry University
Yousry A. El-Kassaby
The University of British Columbia
Deqiang Zhang (DeqiangZhang@bjfu.edu.cn)
Beijing Forestry University https://orcid.org/0000-0002-8849-2366

Research article

Keywords: Poplar, heat stress, photosynthesis, transcriptional regulation, transcription factor (TF), miRNA, gene regulatory network (GRN)

Posted Date: August 6th, 2019

DOI: https://doi.org/10.21203/rs.2.12441/v1

Abstract

Background Photosynthesis has been recognized as a complicated process that is modulated through the intricate regulating network at transcriptional level. However, its underlying mechanism at molecular level under heat stress remains to be understood. Analysis of the adaptive response and regulatory networks of trees to heat stress will expand our understanding of thermostability in perennial plants. In this study, we used a multi-gene network to investigate the regulatory pathway under heat stress, as constructed by a multifaceted approach of combining time-course RNA-seq, regulatory motif enrichment, and expression-trait association analysis. Results By analyzing changes in the transcriptome under heat stress, we identified 77 key photosynthetic genes, of which 97.4% (75 genes) were down-regulated, and these results conformed to the decreased photosynthesis measured values. According to analysis of regulating motif enrichment, these 77 differentially expressed genes (DEGs) had common vital light-responsive elements involved in photosynthesis. When integrating all the differential expressed genes, 5 co-expressed gene modules (1,548 genes) were identified to be significantly correlated with 4 photosynthesis-related traits. Thus, based on this, a three-layered gene regulatory network (GRN) was established, which had included 77 photosynthetic genes (in the bottom layer), 40 TFs/miRNAs (in the second layer), as well as 20 TFs/miRNAs (in the top layer), using a backward elimination random forest (BWERF) algorithm. Importantly, 6 miRNAs and 4 TFs were found to be key regulators in this regulatory pathway, emphasizing the significant roles of TFs/miRNAs in affecting photosynthetic traits. The results imply a functional role for these key genes in mediating photosynthesis under heat stress, demonstrating the potential of combining time-course transcriptome-based regulatory pathway construction, cis-elements enrichment analysis, and expression-trait association approaches to dissect complex genetic networks. Conclusions The heat-responsive pathway in regulating photosynthesis is a multi-layered complex network which is co-controlled by TFs and miRNAs. Our work not only imply a functional role for these key genes in mediating photosynthesis responding to abiotic stress in poplar, but demonstrate time-course transcriptome-based regulatory network construction will facilitate further the genetic network and key nodes examining in plants.

Background

Heat, a kind of frequently-seen environment stress, will restrict the growth and development of plants, as well as crop yield [1, 2]. During their evolution, plants developed responsive mechanisms to adverse stresses, including signal transduction and hormonal regulation [2]. Under heat stress, balanced cell turgor is kept by adjusting the osmotic pressure; meanwhile, the size and elasticity of cells are adjusted by means of protoplasmic tolerance, allowing heat stress tolerance of plants [1, 3, 4]. It is interesting that, heat stress will result in increase in genetic instability, along with more frequent somatic homologous recombination (SHR) [5, 6]. SHR is regulated through chromatin configuration at specific sites [7, 8]; as a result, heat stress may affect genetic stability by modifying DNA recombination and repair accessibility, as well as chromatin configuration [1, 3, 9].

Temporary or persistent high temperature will result in biochemical, physiological, and morphological alterations, which will decrease photosynthesis, finally limiting plant productivity and growth [10, 11]. Photosynthesis is an extremely complicated plant physiological event, which involves a variety of components, such as the electron transport system, photosystems, and the CO_2 reduction pathways, and it is decreased under heat stress [11]. Of the above functions, Photosystem II (PSII) is recognized to be a photosynthetic apparatus component with the highest sensitivity [12]. For example, heat stress will lead to the decreased PSII content while increased Photosystem I (PSI) level in *Populus euphratica* [13]. According to previous studies, moderate heat stress can induce the decreased cyclic electron flow and plastoquinone [14]. Besides, it can also reversibly reduce photosynthesis, while elevated heat stress irreversibly injures photosynthetic apparatus, thus further inhibiting plant growth [11, 12, 15]. As predicted by the Intergovernmental Panel on Climatic Change report, in the end of 21st century the climate on the Earth will be warmed by 2–4°C [16]. Therefore, a comprehensive understanding towards relevant gene expression and photosynthetic physiology in response to heat stress contributes to enhancing plant thermostability and limiting the unfavorable impact of climate changes on the productivity of woody crops.

There are numerous studies examining the role of stress in photosystems, electron transport system, photosynthesis-related enzyme activities, pigments, chlorophyll fluorescence and gas exchange in plant [17–19]. However, a majority of those studies concentrate on plant responses to adapt to the heat stress, while the plant regulatory network in the presence of constant heat stress is rarely mentioned. *Populus,* a kind of rapidly growing woody plant species, is extensively utilized in wood production and landscaping; but its ecological benefits could be greatly impacted by increased temperature. *Populus* have evolved specific physiological mechanisms for adaption to changes in natural environmental conditions [20, 21]. Analyzing the plant regulatory networks and adaptive responses in the presence of heat stress can broaden our knowledge about perennial plant thermostability.

The majority of adaptive response functions by means of gene expression regulation to some extent; as a result, transcript factors responding to heat stress may exert vital parts in the tolerance to abiotic stress [2, 22]. Numerous genes can interact mutually as well as with environment, which play certain roles in the heat stress response [3]. A large array of abiotic stress responsive genes has been identified in plants with microarray and large-scale transcriptome analyses [23]. These genes play a role in cell protection from damage through producing vital metabolic proteins and enzymes, and in regulating gene expression and signal transduction in the presence of stress [2, 3, 24]. Of regulating proteins, transcriptional factors (TFs) have critical parts in converting stress signal perception into expression of stress responding genes, which is achieved through the interaction with *cis*-acting elements different specific stress responding gene promoter regions during signal transduction. Therefore, it can activate signaling cascade in enhancing plant tolerance to harsh environmental conditions [22, 25, 26]. About 7% coding sequences in plant genome can be attributed to TFs, a majority of which are in large gene families in comparison with those in yeasts and animals, like the heat stress transcriptional factors (HSFs) family [2, 22]. It remains unknown about the numbers and expression of genes involved in trees' photosynthesis regulation under

heat stress. As a result, it is of vital importance to characterize and identify genes taking part in plant heat stress tolerance.

Recently, microRNAs (miRNAs), the endogenous short non-coding RNAs, are indicated to exert key parts in the post-transcriptional response to stress in plants [27, 28]. MiRNAs function by the negative regulation of gene expression through enhancing target mRNAs degradation or restraining translation. Numerous miRNAs are found to regulate the plant response to both abiotic and biotic stresses, such as nutrient starvation [29], pathogen invasion [30], cold, salt, and drought [31], and oxidative stresses [32]. Although, miRNAs in heat tolerance studies has been made in plants, a genome-wide identification of miRNAs responsive to consistent heat stress in poplar has not been conducted. Previous studies on poplar have indicated that many miRNAs are differentially expressed [20, 21]. Previous reports on plants under abiotic stress have revealed diverse functions of miRNAs [3, 11, 33]. For example, through regulation of the target genes, rice TEOSINTE BRANCHED1 and a MYB transcription factor, miR139 is up-regulated and involved in process of rice seedling [28]. Similarly, miR393 was found to participate in responding to drought stress in rice via negative regulation of mRNAs encoding the F-box auxin receptor, TIR1 [27]. Therefore, miRNAs genome-wide profiling during consistent heat stress in trees is necessary, so as to comprehensively understand the poplar mechanism in heat stress response and to examine the underlying useful genes in molecular breeding.

In this work, a photosynthesis regulatory network was established responding to heat stress by the transcriptome method coupled with weighted gene co-expression network analysis (WGCNA) analysis and graphic Gaussian model (GGM) algorithm. We show distinct transcriptional changes involving a highly interconnected hierarchically structured network and identified key nodes which response to heat stress in poplar. This study provides insights into the molecular mechanisms and systematic investigation of photosynthesis under heat stress and provides a new strategy for examining the genetic network and key nodes in plants.

Results

Physiological responses of *Populus trichocarpa* to heat stress

To understand the physiological changes of *P. trichocarpa* under heat stress, we examined four photosynthetic characteristics including net photosynthesis (Pn), transpiration rate (Trmmol), leaf internal CO_2 concentration (Ci), and stomatal conductance (Cond) over a time-course under heat stress (0, 4, 8, 12, 24, 36, and 48 h). Overall, we found all four characteristics (photosynthesis rate (Pn), stomatal conductance (Cond), intercellular carbon dioxide concentration (Ci), and transpiration rate (Trmmol)) exhibited significant decrease during the heat stress (Figure 1). For example, after 8 h, we detected a significant decrease in Trmmol (Figure 1d), Ci (Figure 1c), and Cond (Figure 1b), suggesting that heat stress plays a negative role in regulating photosynthesis. However, Cond, Ci and Trmmol showed 2.67,

2.09 and 1.88 fold increase after 4 h of heat stress, respectively. Additionally, Ci, Trmmol, and Cond showed significant positive correlations with each other ($r > 0.85$, $P < 0.01$, Figure 1e). By contrasts, Ci showed significant negative correlations with Pn ($r_{Pn,Ci} = -0.42$, $P < 0.01$), Trmmol ($r_{Pn, Trmmol} = -0.32$, $P < 0.01$) and Cond ($r_{Pn, Cond} = -0.26$, $P < 0.01$).

Profiles of transcripts under heat stress in *P. trichocarpa*

To investigate the transcriptional response under heat stress, we conducted high-throughput RNA-seq (Additional file 1; Average ~24 million reads). In total, 17,003 mRNA genes were detected to be highly expressed (FPKM > = 5, fold-change > 2 and $P < 0.05$), of which, 11,417 were differentially expressed at least at one of the six time points as compared to the control group (Table 1; Additional file 2). These DEGs (differentially expressed genes) are clustered into four co-expression modules by applying K-means clustering algorithm (Figure 2a). Genes of the four clusters exhibited distinct responsive patterns under the heat stress (Figure 2b). For example, the transcript abundance of genes in cluster 4 increased at an early stage and reached a maximum level at 12 h, and then decreased after 36 h. The expression of genes in cluster 1 and 2 remained stable after stress (Figure 2b).

To examine the biological effect of heat responding genes, the functional enrichment analysis was carried out for identifying the over-represented gene ontology (GO) terms (Additional file 3). A total of 15 remarkably common GO terms were identified ($P < 0.05$), all of which were highly related to photosynthetic process (Supplementary Figure 1; Additional file 4). We noticed that a high percentage of genes from photosynthesis, cell wall, and chloroplast and cell division were enriched in the down-regulated genes at 36 h. In total, 117 TF coding genes belonged to 26 families, which were specifically expressed during these six treatment times (Additional file 5). We then used MapMan analysis, which groups heat-responsive genes into hierarchical functional categories based on their putative biological function. As a result, 168 genes were involved in photosynthesis regulation pathway, consisting of light reactions (92), Calvin cycle (41), and photorespiration (35). Of these 168 genes, 152 genes (90.48%) showed decreased expression patterns, as would be expected for decreasing the redox transient efficiency, assembling of *Rubisco* the transport and phosphorylation efficiency in photosynthesis. 76 from the 92 genes in light reaction that participated in key protein complexes were reduced, such as photosystem II (*PSII)*,, photosystem I (*PSI)*,, *F-ATPase,* and cytochrome b6f complex of redox chain (Cyt/b6f) (Figure 3a). In the photorespiration process, *GLDC (*Potri.001G144800), *GLDP (*Potri.006G229300), and other units taking part in converting glycine into methylene-H4-folate, together with *SGAT (*Potri.009G047700 and Potri.001G253300) in the peroxisome reaction with mitochondrion, were also decreased. Such finding indicated that glyoxylate metabolism had been repressed in the presence of heat stress, while enzymes had been deposited in mitochondria. We observed among genes downregulated in 36 h as well as an over-representation of genes involved in secondary metabolism (aspartate family amino acid, anthocyanin, organic acid, and phenylpropanoid biosynthesis) and primary

metabolism (photosynthesis, carboxylic acid, tyrosine, amino sugar metabolisms and nucleic acid binding transcription factor). Above results suggested that heat leads to a reprogramming of primary and secondary metabolism in the poplar transcriptome putatively related to defense activation. Taken together, our result shows a dynamic transcriptional heat-responsive network, which had a negative effect on photosynthetic pathway.

Co-expression patterns responding heat stress in *P. trichocarpa*

To investigate the trait-associated gene regulatory network (GRN) under heat stress, we constructed co-expressed gene matrix via weighted gene co-expression network analysis (WGCNA). A total of 17,003 genes were included in the analysis, and these genes exhibited a high expression dynamic across the heat stress treatments (Supplementary Figure 2). For example, 247 genes of cluster 2, 7, 9, and 10, reached a dip at 36 h but reached a peak at 48 h (Figure 4a-d). Clusters 14 and 15 had a similar expression pattern - early peaks of expression (0 h) and a stable change in later periods (Figure 4e-f). Other clusters expression pattern showed in Supplementary Figure 3. As a result, five co-expression modules of 120 - 4,078 genes were detected to be highly associated with four photosynthesis traits under heat stress ($P < 0.05$; Figure 5; Supplementary Figure 4, 5; Additional file 2). Detailed analyses revealed that these genes are involved in photosynthesis and oxidation reduction processes (Supplementary Figure 6; Additional file 3). Taken together, these results suggested major differences in the transcriptional programs across different heat treatment times. Furthermore, the differences in the transcriptional program at 12 and 36 h may be the determinant on the heat shock responses and photosynthetic regulation.

Heatresponsive genes and miRNAs involved in photosynthesis

To investigate the potential role of miRNAs in regulating photosynthetic, small RNA-seq (average ~13 million reads) were performed (Additional file 6). Our analyses revealed that the DEGs (differentially expressed genes) could be targeted by 163 miRNAs (Additional file 7). After investigating the regulation patterns, 54.63% miRNA/target pairs exhibited significant negative correlations ($r = -0.73$, $P < 0.01$). The highest numbers (8,718 genes) of DEGs were detected at 36 h (Figure 2c, Table 1). Based on this criterion, we identified a total of 168 photosynthesis-related genes could be regulated by 159 miRNAs, of which, 88 are involved in light reaction and could be targeted by 72 miRNAs. Consistently, 50% miRNA/targets showed significant high negative correlations, suggesting that miRNAs play important role in regulating photosynthesis. In addition, in the Calvin cycle, 41 genes could be targeted by 33 miRNAs, and 41.3% showed negative correlations. For example, *RBCS1A (*Potri.015G062100) and *RBCS3B (*Potri.002G007100), protein subunits of *Rubisco,* were downregulated, while miR169 were up-regulated

under heat stress (Figure S7). These findings suggest that a substantial number of the photosynthetic genes can be regulated by miRNAs under heat stress.

Genetic networks involved in photosynthesis response to heat stress

Combined with the weighted gene co-expression network (WGCNA) and MapMan analyses, we detected 77 differentially expressed genes (DEGs) involved in regulating photosynthetic pathways like electric transduction, carbon assimilation, and light reaction (Additional file 8). We identified 42 *cis*-regulatory motifs including some light-responsive elements that were enriched in the promoters of the 77 DE photosynthetic genes ($P < 0.05$), raising the possibility that some key regulators involved in this process. To further explore the key factors involved in regulating photosynthesis, we constructed a multilayers hierarchical gene regulatory networks that govern photosynthetic pathways. As a result, 77, 40 and 20, genes/miRNAs pairs were found to be located at the first (bottom), second (middle), and third layers (top), respectively (importance score > 8.5, $P < 0.05$; Figure 6a). Consistently, 30 correlations are detected by a gene-gene correlation matrix based on the RT-qPCR result with a 0.72 ($P < 0.001$) correlation coefficient (Supplementary Figure 8).

Thirteen key TFs, such as Dof3, MYB22, ZF-HD3, ERF6, and MIKC-MAD4, were detected to regulate 74 downstream photosynthetic genes. HsfA1, a master regulator of transcriptional regulation under heat stress, induce the expression of the downstream transcription factors, such as DREB2A, MIKC-MAD, and NAC. In addition, DREB2A could induce the transcription of 30 downstream target genes. MiRNAs are also emerging as factors involved in regulating photosynthesis. Of these, miR1444d and miR396a could regulate 32 and 34 downstream photosynthetic genes, respectively, such as *PETC, FD, PGRL1,* and *PETE,* which are involved in electron transfer. Notably, the targets of some miRNAs were TFs, which amplified the effect of miRNAs through hierarchical regulation. For example, miR396 could regulate a MYB transcription factor (MYB22) and a bZIP DNA binding protein (bZIP28). Consistent with this, miR1444 were functionally significant miRNAs targeting polyphenol oxidase (*PPO)* genes for cleavage which started 2 nt upstream of precursor, resulting in differential regulation of PPO targets [34]. Notably, 19 downstream DEGs could be regulated by both key TFs and miRNAs. For example, MYB22 and miR396a were found to regulate 19 common DEGs (Figure 6b). Overall, the heat-responsive pathway in regulating photosynthesis is a multi-layered complex network which is co-controlled by TFs and miRNAs.

Discussion

Negative transcriptional effects of heat stress on photosynthesis

Under global climatic change, elevated temperature is seen as the most serious threat to crop production [35–37]. Heat stress, whether transient or continuous, could cause biochemical, physiological, and molecular changes that adversely affect tree growth and productivity by reducing photosynthesis [38–40]. Photosynthesis in plants is composed of two interconnected biological functions, CO_2 transport and biochemical processes [41]. Studies on the fine temporal scale (i.e., hours) of the poplar response to heat are virtually rare, specifically those dealing with understanding of changes in photosynthesis under heat stress. Here, we provide the first glimpse into the regulation of photosynthesis under heat stress.

Previous studies have reported that heat stress induced cleavage and aggregation of PSII reaction center (RC) proteins, resulting in negative effects on photosynthesis [42, 43]. High temperature could also inhibited photosynthesis by several mechanisms including deactivation of Rubisco, activation of NADP-malate dehydrogenase and an acceptor-side limitation imposed on photosynthetic electron transport in cotton, grapevine, tobacco and other plants [44–46]. Our study demonstrated that three important photosynthetic characteristics including transpiration rate (Trmmol), leaf internal CO_2 concentration (Ci), and stomatal conductance (Cond) were significantly decreased, suggesting that heat stress has permanent adverse effects on photosynthesis; however, no appreciable effect was observed for net photosynthesis (Pn). Previous studies investigated the main cause of reduced Pn and concluded that it may be caused by the decrease of Ci and Cond [11]. If both Cond and Ci simultaneously increase, increasing stomatal conductance will mainly limit Pn [40, 42]. High temperature stress causes multi-step injuries to the photosynthetic machinery (PM), and the enzymes of the Calvin-Benson cycle are heat labile [42]. Therefore, the carbon absorption system shows high sensitivity to the increased temperature, which is greatly suppressed under moderate heat stress [12, 13]. The reduced Rubisco activity in the presence of moderate heat stress is related to photosynthetic loss [43]. Heat will induce alterations in Chl-protein complex structures and inactive enzyme activities, which have constituted the heat stress effects, eventually contributing to decreasing Pn. Heat stress at 35–45 ℃ can result in generally reorganized thylakoid membranes and reduced membrane stacking [47]. The above structural changes resulted in a modest decrease of Cond and Ci, which might cause Pn to decrease.

A model for the heat stress-responsive pathway in regulating photosynthesis

Previous studies have demonstrated extensive changes in the transcriptome under heat stress [1, 3, 42]. Nonetheless, the alterations of gene regulation network in woody plant photosynthetic tissues have been rarely mentioned. Here, by using dynamic transcriptome data, this paper had demonstrated numerous negative and positive transcriptional regulators, which might function as the transcriptional cascade to activate downstream target gene expression in the photosynthetic pathways: light reaction, photorespiration, and Calvin cycle. Indeed, several *cis*-elements were co-occurred in the promoter regions of the down-stream photosynthetic genes. A total of 42 *cis*-elements were enriched in the promoters of 77 downstream photosynthetic DEGs, such as the TATA and CAAT boxes, stress responding elements

(BIHD1OS and EBOXBNNAPA), light responding elements (GATABOX and SORLIP1AT), hormone responding elements (WRKY71OS and MYB1AT), organ specific elements (POLLEN1LELAT52 and GGNCC), the phosphate-starvation responding element, and the sulfur responding element. These results thus provide potential for studying the heat-responsive genes involved in photosynthesis.

The high temporal-resolution that transcriptome profiling data generated in our study provided good opportunity to identifying key regulators, which is also highly informative for inferring gene function and understanding the genetic control of regulating photosynthesis under heat stress. In the present study, we identified 4 TFs and 6 miRNAs, which are key players in regulating photosynthesis. In upstream regulating cascade, heat stress can derepress the signal transduction pathway through promoting proteolysis of the negatively regulated miRNAs through interaction for releasing TFs [3]. MYB22, a key TF in the regulation network, known to be involved in the maturation program in development under heat stress [48, 49]. MiR396, also a key node detected in our network, could repress the expression of *PIF1* and further impact the transcription of *SBPase* [50, 51]. For downstream target genes, *LHCA, LHCB, RBCS,* and *ATPase* were repressed under heat stress across different treatment times, supporting the idea that upstream receptors and signaling components may respond at different heat stress treatment times under. Thus, taking advantage of the high temporal-resolution transcriptome, we could propose a model for the heat stress-responsive pathway in regulating photosynthesis (Figure 7).

A novel approach for gene regulatory network construction

It has been proved that, it is useful to apply gene expression profiling data in constructing co-expression network, and in performing network decomposition and analysis in biological study. Combining the expression-traits association method, *cis*-elements enrichment, and multilayered hierarchical gene regulatory network (ML-hGRN) construction approaches to discovery key players controlling photosynthetic genes is particularly important. Weighted correlation network analysis (WGCNA) is distinctly different from previously mentioned methods in that the former defines a network persistently linking all variables before clustering variables with high co-expression within the modules defined flexibly [52–54]. It could explicitly define all of the relationships between metabolites at multiple scales, facilitates identifying essential downstream processes that are tightly related to traits. In our study, we first identified 1,548 downstream heat-responsive genes. Then, based *cis*- element, we further reduced false-positives. Following stringent filtration, many genes are excluded from the eventual datasets; which do not stand for the direct active players in this pathway. Thus, 77 downstream photosynthetic genes and 442 upstream regulators, including 279 TFs and 163 DE miRNAs remained. Finally, based on the downstream target genes, and upstream regulators (TFs and miRNAs), a multilayered hierarchical gene regulatory network (ML-hGRN) was constructed. In this ML-hGRN, MYB22, miR396a, miR1444d, DREB2A, and ZF-HD3 were identified as key nodes, which were supported by previous studies. For example, DREB2A were reported to bind to a *cis*-acting dehydration-responsive element (DRE) and activated the

expression of *Hsp70, AREB1,* and *ATEM6* in response to drought and salt stress [24, 55]. MiR396a, regulators of stress resistant processes, implicated to be key players in response to heat stress [33, 50]. Therefore, this multifaceted approach identified key genes in regulating photosynthesis, and serves as a model for interrogating complex signaling networks.

Conclusions

Heat stress made extensive changes in the transcriptome and caused biochemical, physiological, and molecular changes that adversely affect plant growth. Although a large amounts of genes have been identified in many plant species, little attention has been paid to changes in gene regulation network in photosynthetic tissues of woody plants. Here we combined the expression-traits association method, cis-elements enrichment, and multilayered hierarchical gene regulatory network (ML-hGRN) approaches to discovery key players controlling photosynthetic genes. A total of 10 key nodes (4 TFs, 6miRNAs) were identified which regulating 77 essential photosynthetic pathway genes under heat stress. Moreover, the expression pattern of 77 photosynthetic genes at different treatment points in response to heat stress revealed that different members might play specific roles in responding heat stress. Interestingly, the expression profiling of photosynthetic genes showed similar down-regulating pattern under heat stress across different time points, suggesting stress-induced genes might have multiple functions in down-regulating photosynthesis and responding heat stress. Furthermore, the heat-responsive pathway in regulating photosynthesis is a multi-layered complex network which is co-controlled by TFs and miRNAs. Importantly, MYB22, miR1444 and miR396a might make significant roles in responding to abiotic stresses, particularly in heat and drought. Taken together, the results imply a functional role for these key genes in mediating photosynthesis responding to abiotic stress, demonstrating time-course transcriptome-based regulatory network construction will facilitate further the genetic network and key nodes examining in plants.

Materials And Methods

Plant Materials

Ramets of *P. trichocarpa* (one genotype) were used and collected by Dr. Yiyang Zhao, from a greenhouse located in Beijing Forestry University, Beijing, China (40°0'N, 116°08'E). The specimen was deposited in the Beijing Forestry University Herbarium (voucher 00080269). The samples were treated according to the method of Zhang et al. (2010). Ramets were transplanted to the nutrition blocks supplemented with common garden soil within a period of 30 days. Subsequently, samples that had identical growth degree were transplanted to the nutrition pots (with the diameter of 30 cm) supplemented with identical amount of common garden soil separately. Then, *P. trichrocarpa* ramets at the age of 1 year had been planted at the 16 h light and 8 h dark cycle. Subsequently, seedlings had been exposed to 40 °C temperature for with 4, 8, 12, 24, 36, and 48 h, and samples that grew under 25 °C had been utilized as controls. The relative

humidity was determined at 50% ± 1, which was maintained in the measuring process. All treatment groups, such as control, included 3 biological replications (ramets).

Measurement of photosynthetic rates

From August 18th–24th, 2017, the No.4 completely expanding leaves were collected from all the three ramets under every treatment to measure the photosynthetic rate through the portable photosynthesis system (LI–6400; Li-Cor Inc., Lincoln, NE, USA). In order to fully induce photosynthesis, every sample was subjected to 30 min of illumination at saturated photosynthetic photon flux density (PPFD) from the light emitting diode (LED) light source prior to measurements. Afterwards, the transpiration rate (Trmmol), net photosynthetic rate (Pn), stomatal conductance (Cond), and intercellular CO2 concentration (Ci) in leaf had been determined simultaneously. Each measuring parameter followed the methods mentioned by Chen et al. [56].

Construction, processing, and annotation of the *P. trichrocarpa* cDNA libraries

Leaves were harvested from 1-year-old *P. trichrocarpa* at 0, 4, 8, 12, 24, 36 and 48 hours after 40 °C heat treatment. The completely expanding leaves were collected, immediately put into liquid nitrogen, and preserved under –80 °C until further use. Total RNA was extracted according to the modified hexadecyl trimethyl ammonium bromide (CTAB) assay mentioned by Chang et al. (1993); to be specific, isopropanol rather than lithium chloride was used for RNA precipitation, and the genomic DNA was eliminated using DNase. The quality of RNA was evaluated using Agilent Bioanalyzer 2100 (Agilent Technologies, Santa Clara, CA, USA), Qubit 2.0 Fluorometer (Invitrogen, Life Technologies, CA, USA), and NanoDrop ND–2000 (Thermo Fisher Scientific, Waltham, MA, USA). Afterwards, high-quality RNA had been utilized in building the cDNA library in accordance with TruSeq RNA Sample Preparation instruction (Illumina, San Diego, CA, USA).

Following analysis, those samples that had the OD 260/280 ratio of 1.9–2.1 and the OD 260/230 ratio of 1.8–2.2 would be selected for subsequent use. Paired-end sequencing was performed by Novogene (Beijing, China) on an Illumina HiSeq 4000 platform (Illumina), generating 150-bp paired-end reads using TruSeqPEClusterKitv3-cBot-HS (Illumina) according to the manufacturer's instructions and the strand-specific libraries were sequenced. Quality control and other downstream analyses were performed on the cleaned data. In this step, clean data (clean reads) had been acquired through eliminating adapter- and ploy-N-containing reads, as well as the low-quality reads out of the raw material. The clean reads had then be mapped into reference genome of *P. trichrocarpa* with Bowtie2 program. The filtered high-quality reads were mapped on the *P.trichrocarpa* genome using TopHat (v2.0.0) with default parameters. Feature Countsv1.5.0-p3 had been utilized for counting reads that were mapped into every gene; afterwards, FPKM was computed for all genes according to gene length and reads that were mapped into the specific

gene. The mapped results were then processed using Cufflinks (v2.0.2) for obtaining FPKM for every *Populus* gene of every sample with default parameters. Then, the correlations among biological replicates had been examined through computing the Spearman correlation coefficient. Cuffdiff was used to determine the differential expression among various samples. Genes that had > = 2-fold change and the *P*-value of < = 0.05 [adjusted with the false discovery rate (*Q*-value)] had been deemed as the significantly differentially expressed genes (DEGs).

Small RNA (sRNA) library construction, annotation and processing for *P. trichrocarpa*

Total RNA sample, which was identical to that utilized in transcriptomic sequencing, was used for constructing sRNA libraries. In brief, the sRNA pieces (18–30 nt) had been isolated, which was then subjected to polyacrylamide gel electrophoresis (PAGE) for purification. Afterwards, the sRNA segments had been ligated to 3′ and 5′ adaptors using T4 RNA ligase. Then, the adaptor-ligated sRNAs had been subjected to transcription into single strand cDNA, followed by PCR amplification for 12 cycles. Later, samples coded by index were clustered using the cBot Cluster Generation System by the TruSeq SR Cluster Kit v3-cBot-HS (Illumia) in accordance with manufacturer protocols. Following cluster production, all library preparations had been sequenced through the Illumina Hiseq 2500 platform to generate the 50 bp single end reads.

Identifying differentially expressed miRNAs and analyzing the specific targets

In each sample, each read was standardized to be the transcripts per million (TPM) based on all sequenced reads. Typically, miRNAs that had the $\log_2$ fold change of > = 1.0 or the $\log_2$ fold change of < = −1.0, FDR < = 0.05, and $P < 0.05$ had been deemed as the significantly differentially expressed miRNAs. Specifically, fold change was calculated as follow, fold change = |TPM ratio| (treatment/control). Then, psRNATarget (http://plantgrn.noble.org/psRNATarget/) with accessibility of parameter target at 25.0, together with the complementarity scoring length at 20, had been utilized for predicting the candidate target genes for a total of 179 miRNAs. Typically, targets were identified using the transcript library of *P. trichocarpa* preserved within Phytozome database v.3.0 (http://www.phytozome.net/poplar). Moreover, the scoring systems for the mismatches during the interaction between miRNA and mRNA had been assigned below: 0 suggested a complementary pair; 0.5 indicated G:U wobble; 1 stood for other mismatches; 2 represented every opening gap; while 0.5 was indicative of the extending gap [57]. Moreover, the miRNA/mRNA duplexes that had the score of < = 2.0 had been regarded to be the highly confident target-miRNA interactions. Accordingly, candidate targets that had the fold change of > = 2, $Q < 0.05$ and $P < 0.01$ had been deemed with significant differential expression. Additionally, to examine the relationship of expression between miRNAs and target genes, pairwise Pearson correlations between

targets and miRNAs had been computed to explore the association of miRNA expression with target gene expression. All *P*-values had been adjusted by the false discovery rate (FDR; $P < 0.01$, $Q < 0.05$). The R software (R Development Core Team, 2012) was used for calculation.

GO and pathway enrichment analysis

The AgriGO analysis approaches (http://bioinfo.cau.edu.cn/agriGO/) were utilized for enrichment analysis of gene set. The precise annotation data were obtained based on the Kyoto Encyclopedia of Genes and Genomes (KEGG, http://www.genome.jp/kegg), as well as PopGenie (http://popgenie.org). Then, the enrichment *P*-value was computed for every represented GO term, which was also adjusted according to the Benjamini Hoschberg error correction approach. Afterwards, GO terms that had adjusted (after FDR adjustment) $P \leq 0.05$ had been regarded as significantly enriched. Furthermore, the MapMan (Version: 3.5.1) categories were used for pathway enrichment analysis of various gene sets (significance value < = 0.05).

Co-expression network analysis for construction of modules

For co-expression network analysis, the weighted gene co-expression network analysis (WGCNA) [58] package had been employed. According to the $\log_2$ (1 + FPKM) numbers, the pairwise Spearman correlation coefficient matrix had been generated among different gene pairs, which was then converted into the adjacency matrix (the connection strength matrix) through the following formula: connection strength (namely, adjacency value) = $|(1 + \text{correlation})/2|^{\beta}$, where β represented the correlation matrix soft threshold and it rendered a higher weight to the strongest correlation in the meantime of keeping connectivity between genes. Additionally, the β-value at 12 had been chosen according to scale-free topological criteria from Horvath and Zhang (2005). Afterwards, the obtained adjacency matrix would be transformed into the topological overlap (TO) matrix (TOM) using the TOM similarity algorithm; then, genes had been clustered hierarchically according to the TO similarity. Hierarchal clustering dendrogram was cut by dynamic tree-cutting algorithm, and then modules would be defined following branch decomposition/combination, so as to obtain the fixed cluster quantity [58]. In every module, PCA was computed through the summary profile (namely, module eigengene, ME). Besides, modules that had greater TO values (average TO of all genes within one specific module) than those of modules consisting of genes selected randomly would be preserved. Later, Cytoscape [59, 60] was used for GO enrichment analysis for all modules, as described above.

Identification and co-expression analysis of cis-regulatory elements and TFs

The transcription modules were predicted in accordance with the methods by Belmonte et al. (2013) after certain modifications. In order to examine over-represented DNA motifs within the heat responding photosynthetic DEGs, promoter sequences (2 kb) in front of the 5′ terminal in every annotated transcriptional unit during *Populus* annotation had been collected. Then, the identified promoter elements of plants, together with the corresponding annotations, had been derived from PlantPAN 2.0 [61]. Moreover, the promoter sequences from each *Populus* gene had been utilized to be the background, and hypergeometric test was carried out to detect the over-represented motifs. A co-expression analysis (Pearson correlation) was then performed using the Hmisc 4.1.0 package in R for detecting the correlation networks of gene expression, and all criteria below were used for gene filtering: $|r| >= 0.6$ and $P <= 0.05$. The networks were drawn using Cytoscape [59, 60].

Multilayered hierarchical gene regulatory network (ML-hGRN) construction using a backward elimination random forest (BWERF) algorithm

The sequences of the 77 genes (Additional file 8) known to be directly involved in photosynthesis which were classified as light reaction, Calvin cycle and photorespiration based on MapMan and WGCNA analyses, and the PlantPAN2.0 was utilized to evaluate the *cis*-regulatory elements in every promoter sequence (2 kb in length) [61]. O the basis of 80% confidence, the above motifs had been utilized in identifying the 279 TFs that potentially targeted the photosynthetic genes using PlantPAN2.0. Transcriptional profiles of these TFs and photosynthesis genes were obtained from the transcriptome data, and those genes were retained for further analysis. A ML-hGRN had been established according to the BWERF algorithm, among which, 77 photosynthetic genes were in bottom layer, while 163 miRNAs and 279 TFs were within regulating layer [62]. Additionally, a three-layered GRN had also been constructed using 32 miRNAs and 18 TFs potentially regulating the 77 photosynthesis genes either directly or indirectly. Cytoscape was used to draw the network [59].

Quantitative realtime PCR (qRTPCR) analysis

The 7500 Fast Real-time PCR System (Applied Biosystems, Waltham, MA, USA) was used for RT-PCRs by Light Cycler-FastStart DNA master SYBR Green I kit (Roche). The Primer Express 3.0 (Applied Biosystems, Waltham, MA, USA) was employed to design each primer pair of purative gene (Additional file 9). Each RT-qPCR amplification was performed according to the standard reaction procedure in triplicate biological and technical replications. Then, the amplified fragment specificity had been examined by the produced melting curve. The Opticon Monitor Analysis Software 3.1 tool (Bio-Rad) was adopted to analyze the produced real-time data. To measure the expression of photosynthetic genes, the poplar *Actin* gene (accession no. EF145577) had been utilized for internal reference. The relative miRNA level would be

measured and normalized based on 5.8S rRNA according to the method from Song et al. (2013). Moreover, the total RNA was reversely transcribed into the cDNA templates used in reactions.

Abbreviations

GRN: gene regulatory network; transcription factor (TF); BWERF: backward elimination random forest (BWERF); GGM: graphic Gaussian model; cDNA: complementary deoxyribonucleic acid; PCR: Polymerase Chain Reaction kg: kilogram cm: centimeter; DEG: differentially expressed gene; TPM: transcripts per million; FC: fold change; GO: Gene ontology; ML-hGRN: multilayered hierarchical gene regulatory network; WGCNA: weighted gene co-expression network analysis; ME: module eigengene; TO: topological overlap; Pn: net photosynthetic rate; Trmmol: transpiration rate; Ci: leaf intercellular CO2 concentration; Cond: stomatal conductance; PPFD: photosynthetic photon flux density; LED: light-emitting diode; PPO: polyphenol oxidase; PM: photosynthetic machinery; HSF: heat stress transcription factor; DRE: dehydration-responsive element;

Declarations

Ethics approval and consent to participate

Not applicable.

Consent for publication

Not applicable.

Availability of data and material

Raw data are available for download at the BIGD Genome Sequence Archive under accession number CRA001776.

Competing interests

All authors declare that they have no competing interests.

Funding

The current study had been funded by the Project of National Natural Science Foundation of China (Nos. 31500550 and 31670333). The funding body had no contribution in the design of the study and

collection, analysis, and interpretation of data and in writing the manuscript.

Authors' contributions

All authors contributed substantially to the study and manuscript. DQZ was responsible for experimental design, obtaining financial support for the study, and project supervising. YYZ was in charge of experiment implementation, data collection and analysis, and manuscript writing. JBX, WJX, SSC, and YAE revised the manuscript and provided valuable suggestions to the manuscript. All authors read and approved the manuscript.

Acknowledgements

Not applicable.

References

1.Qu AL, Ding YF, Jiang Q, Zhu C. Molecular mechanisms of the plant heat stress response. Biochemical and Biophysical Research Communications. 2013;432(2):203–207.

2.Guo M, Liu JH, Ma X, Luo DX, Gong ZH, Lu MH. The plant heat stress transcription factors (HSFs): structure, regulation, and function in response to abiotic stresses. Frontiers in Plant Science. 2016;7(273):114.

3.Krishna P. Plant responses to heat stress. Springer Berlin Heidelberg. 2003.

4.Liu J, Feng L, Li J, He Z. Genetic and epigenetic control of plant heat responses. Front Plant Sci. 2015;6:267.

5.Pecinka A, Rosa M, Schikora A, Berlinger M, Hirt H, Christian H, Scheid OM. Transgenerational stress memory is not a general response in Arabidopsis. Plos One. 2009;4(4):e5202.

6.Lebel EG, Masson J, Bogucki A, Paszkowski J. Stress-induced intrachromosomal recombination in plant somatic cells. Proceedings of the National Academy of Sciences of the United States of America. 1993;90(2):422–426.

7.Takeda K. Continuous regional arterial infusion of protease inhibitor and antibiotic for severe acute pancreatitis. Nihon Rinsho Japanese Journal of Clinical Medicine. 2004;62(11):2101.

8.Kirik A, Pecinka A, Wendeler E, Reiss B. The chromatin assembly factor subunit FASCIATA1 is involved in homologous recombination in plants. Plant Cell. 2006;18(10):2431–2442.

9.Chen H, Hwang JE, Lim CJ, Kim DY, Lee SY, Lim CO. Arabidopsis DREB2C functions as a transcriptional activator of HsfA 3 during the heat stress response. Biochemical and Biophysical Research Communications. 2010;401(2):238–244.

10.Kosma DK, Jenks MA. Eco-physiological and molecular genetic determinants of plant cuticle function in drought and salt stress tolerance. Springer Netherlands. 2007.

11.Ashraf M, Harris PJC. Photosynthesis under stressful environments: an overview. Photosynthetica. 2013;51(2):163–190.

12.Berry J, Bjorkman O. Photosynthetic response and adaptation to temperature in higher plants. Annual Revplphysiol. 1980;31(1):491–543.

13.Ferreira S, Hjerno K, Larsen M, Wingsle G, Larsen P, Fey S, Roepstorff P, Pais M. Proteome profiling of *Populus euphratica* Oliv. Upon heat stress. Ann Bot. 2006;98(2):361–377.

14.Schrader SM, Wise RR, Wacholtz WF, Ort DR, Sharkey TD. Thylakoid membrane responses to moderately high leaf temperature in Pima cotton. Plant Cell & Environment. 2010;27(6):725–735.

15.Sharkey TD, Zhang R. High temperature effects on electron and proton circuits of photosynthesis. Journal of Integrative Plant Biology. 2010;52(8):712–722.

16.Eitzinger J, Orlandini S, Stefanski R, Naylor REL. Climate change and agriculture: introductory editorial. The Journal of Agricultural Science. 2010;148(5):499–500.

17.Wise RR., Olson AJ, Schrader SM, Sharkey TD. Electron transport is the functional limitation of photosynthesis in field-grown pima cotton plants at high temperature. Plant Cell & Environment. 2010;27(6):717–724.

18.Pengmin L, Lailiang C, Huiyuan G, Chuangdao J, Tao P. Heterogeneous behavior of PSII in soybean (*Glycine max)* leaves with identical PSII photochemistry efficiency under different high temperature treatments. Journal of Plant Physiology. 2009;166(15):1607–1615.

19.Mathur S, Allakhverdiev SI, Jajoo A. Analysis of high temperature stress on the dynamics of antenna size and reducing side heterogeneity of Photosystem II in wheat leaves (*Triticum aestivum)*.. Biochimica Et Biophysica Acta. 2011;1807(1):22–29.

20.Zhang D, Du Q, Xu B, Zhang Z, Li B. The actin multigene family in *Populus:* organization, expression and phylogenetic analysis. Molecular Genetics & Genomics. 2010;284(2):105–119.

21.Brunner AM, Busov VB, Strauss SH. Poplar genome sequence: functional genomics in an ecologically dominant plant species. Trends in Plant Science. 2004;9(1):49–56.

22.Saibo NJM, Lourenco T, Oliveira MM. Transcription factors and regulation of photosynthetic and related metabolism under environmental stresses. Annals of Botany. 2009;103(4):609–623.

23.Nakashima A, Kobayashi Y, Ogawa Y, Hayakawa Y. Modeling of rebound phenomenon between ball and racket rubber with spinning effect. In: Iccas-Sice. 2009;2295–2300.

24.Yoshida T, Sakuma Y, Todaka D, Maruyama K, Qin F, Mizoi J, Kidokoro S, Fujita Y, Shinozaki K, Yamaguchi-Shinozaki K. Functional analysis of an Arabidopsis heat-shock transcription factor HsfA3 in the transcriptional cascade downstream of the DREB2A stress-regulatory system. Biochem Biophys Res Commun. 2008;368(3):515–521.

25.Lam-Son Phan T, Kazuo N, Yoh S, Yuriko O, Feng Q, Simpson SD, Kyonoshin M, Yasunari F, Kazuo S, Kazuko YS. Co-expression of the stress-inducible zinc finger homeodomain ZFHD1 and NAC transcription factors enhances expression of the ERD1 gene in Arabidopsis. Plant Journal. 2010;49(1):46–63.

26.Akhtar MW, Kim MS, Adachi M, Morris MJ, Qi X, Richardson JA, Bassel-Duby R, Olson EN, Kavalali ET, Monteggia LM. In vivo analysis of MEF2 transcription factors in synapse regulation and neuronal survival. Plos One. 2012;7(4):485–491.

27.Lewis R, Mendu V, Mcnear D, Tang G. Roles of microRNAs in plant abiotic stress. 2010:357–372.

28.Jeong DH, Green PJ. The role of rice microRNAs in abiotic stress responses. Journal of Plant Biology. 2013;56(4):187–197.

29.Fujii H, Chiou TJ, Lin SI, Aung K, Zhu JK. A miRNA involved in phosphate-starvation response in Arabidopsis. Current Biology. 2005;15(22):2038–2043.

30.Koh S, Somerville S. Show and tell: cell biology of pathogen invasion. Current Opinion in Plant Biology. 2006;9(4):406–413.

31.Kim JM, Sasaki T, Ueda M, Sako K, Seki M. Chromatin changes in response to drought, salinity, heat, and cold stresses in plants. Front Plant Sci. 2015;6:114.

32.Hwang JE, Chan JL, Chen H, Je J, Song C, Lim CO. Overexpression of Arabidopsis dehydration-responsive element-binding protein 2C confers tolerance to oxidative stress. Molecules & Cells. 2012;33(2):135.

33.Akdogan G, Tufekci ED, Uranbey S, Unver T. MiRNA-based drought regulation in wheat. Funct Integr Genomics. 2016;16(3):221–233.

34.Cui XN, Yuan LC, Wu XY, Su XJ. MiR1444a is involved in the response of *Populus trichocarpa* to zinc stress. Scientia Sinica. 2012;42(10):850.

35.Feddes RA. Water, heat and crop growth. H Veenman and Zonen NV, Wageningen.1971.

36.Levis S. Crop heat stress in the context of earth system modeling. IEEE transactions on neural systems & rehabilitation engineering. A Publication of the IEEE Engineering in Medicine & Biology Society. 2014;9(6):886–898.

37.Ma X, Peng H, Mao W, Li W, Sun Q. Evaluation of heat tolerance in crop. Chinese Bulletin of Botany. 2004.

38.Allen CD, Macalady AK, Chenchouni H, Bachelet D, Mcdowell N, Vennetier M, Kitzberger T, Rigling A, Breshears DD, Hogg EH. A global overview of drought and heat-induced tree mortality reveals emerging climate change risks for forests. For Ecol Manage. 2010;259(4):660–684.

39.Ledezma GA, Bejan A, Errera MR. Constructal tree networks for heat transfer. Journal of Applied Physics. 1997;82(1):89–100.

40.Teskey R, Wertin T, Bauweraerts I, Ameye M, Mcguire MA, Steppe K. Responses of tree species to heat waves and extreme heat events. Plant Cell & Environment. 2015;38(9):1699–1712.

41.And GDF, Sharkey TD. Stomatal conductance and photosynthesis. Annu Rev Plant Physiol. 1982;33(33):317–345.

42.Allakhverdiev SI, Kreslavski VD, Klimov VV, Los DA, Carpentier R, Mohanty P. Heat stress: an overview of molecular responses in photosynthesis. Photosynthesis Research. 2008;98(1–3):541–550.

43.Sharkey TD. Effects of moderate heat stress on photosynthesis: importance of thylakoid reactions, rubisco deactivation, reactive oxygen species, and thermotolerance provided by isoprene. Plant Cell & Environment. 2005;28(3):269–277.

44.Salvucci ME, Crafts-Brner SJ. Inhibition of photosynthesis by heat stress: the activation state of Rubisco as a limiting factor in photosynthesis. Physiologia Plantarum. 2010;120(2):179–186.

45.Von CS. Increased heat sensitivity of photosynthesis in tobacco plants with reduced rubisco activase. Photosynthesis Research. 2001;67(1–2):147–156.

46.Wang LJ, Fan L, Loescher W, Duan W, Liu GJ, Cheng JS, Luo HB, Li SH. Salicylic acid alleviates decreases in photosynthesis under heat stress and accelerates recovery in grapevine leaves. Bmc Plant Biology. 2010;10(1):34.

47.Genji K, Huamin Z, Smith JL, Cramer WA. Structure of the cytochrome b6f complex of oxygenic photosynthesis: tuning the cavity. Science. 2003;302(5647):1009–1014.

48.Chiu RS, Nahal H, Provart NJ, Gazzarrini S. The role of the Arabidopsis FUSCA3 transcription factor during inhibition of seed germination at high temperature. BMC Plant Biol. 2012;12:15.

49.Guo X, Hou X, Fang J, Wei P, Xu B, Chen M, Feng Y, Chu C. The rice gd1, encoding a B3 domain transcriptional repressor, regulates seed germination and seedling development by integrating GA and carbohydrate metabolism. The Plant journal: for cell and molecular biology. 2013;75(3):403–416.

50.Bao M, Bian H, Zha Y, Li F, Sun Y, Bai B, Chen Z, Wang J, Zhu M, Han N. MiR396a-mediated basic helix-loop-helix transcription factor bHLH74 repression acts as a regulator for root growth in Arabidopsis seedlings. Plant & Cell Physiology. 2014;55(7):1343–1353.

51.Wang L, Gu X, Xu D, Wang W, Wang H, Zeng M, Chang Z, Huang H, Cui X. MiR396-targeted AtGRF transcription factors are required for coordination of cell division and differentiation during leaf development in Arabidopsis. Journal of Experimental Botany. 2011;62(2):761.

52.Botía JA, Vandrovcova J, Forabosco P, Guelfi S, D'Sa K, Hardy J, Lewis CM, Ryten M, Weale ME. An additional k-means clustering step improves the biological features of WGCNA gene co-expression networks. BMC Systems Biology. 2017;11(1).

53.Di Y, Chen D, Yu W, Yan L. Bladder cancer stage-associated hub genes revealed by WGCNA co-expression network analysis. Hereditas. 2019;156(1):7.

54.Zhai X, Xue Q, Liu Q, Guo Y, Chen Z. Colon cancer recurrence associated genes revealed by WGCNA coexpression network analysis. Molecular Medicine Reports. 2017;16(5).

55.Sakuma Y, Maruyama K, Osakabe Y, Qin F, Seki M, Shinozaki K, Yamaguchi-Shinozaki K. Functional analysis of an *Arabidopsis* transcription factor, DREB2A, involved in drought-responsive gene expression. Plant Cell. 2006;18(5):1292–1309.

56.Chen F, Chen L, Zhao H, Korpelainen H, Li C. Sex-specific responses and tolerances of *Populus cathayana* to salinity. Physiologia Plantarum. 2010;140(2):163–173.

57.Jones-Rhoades MW, Bartel DP. Computational identification of plant microRNAs and their targets, including a stress-induced miRNA. Molecular Cell. 2004;14(6):787–799.

58.Langfelder P, Zhang B, Horvath S. Defining clusters from a hierarchical cluster tree: the dynamic tree cut package for R. Bioinformatics. 2008;24(5):719–720.

59.Shannon P, Markiel A, Ozier O, Baliga NS, Wang JT, Ramage D, Amin N, Schwikowski B, Ideker T. Cytoscape: a software environment for integrated models of biomolecular interaction networks. 2003.

60.Smoot ME, Ono K, Ruscheinski J, Wang PL, Ideker T. Cytoscape 2.8: new features for data integration and network visualization. 2011.

61.Chow CN, Zheng HQ, Wu NY, Chien CH, Huang HD, Lee TY, Chianghsieh YF, Hou PF, Yang TY, Chang WC. PlantPAN 2.0: an update of plant promoter analysis navigator for reconstructing transcriptional regulatory networks in plants. Nucleic Acids Research. 2016;44(Database issue):D1154-D1160.

62.Deng W, Zhang K, Busov V, Wei H. Recursive random forest algorithm for constructing multilayered hierarchical gene regulatory networks that govern biological pathways. PLoS One. 2017;12(2):e0171532.

Tables

Table 1 Differentially expressed genes (DEGs) in *P. trichocrapa* in response to heat stress condition

Time	4h	8h	12h	24h	36h	48h
Total DEGs	4671	4678	6360	5505	8718	6158
Down-regulated	2304	2425	3125	2717	4590	3033
Up-regulated	2367	2253	3235	2788	4128	3125

Table 2 Top 10 key nodes in network ranked by MCC method

Rank	Name	Score
1	MYB22	40
2	Nin-like	39
3	ptc-miR1444d	38
4	ptc-miR396a	34
4	BBR-BPC4	34
6	ptc-miR160a	33
6	ptc-miR156a	33
8	ptc-miR159d	31
9	ptc-miR476a	30
10	ZF-HD3	29

Figures

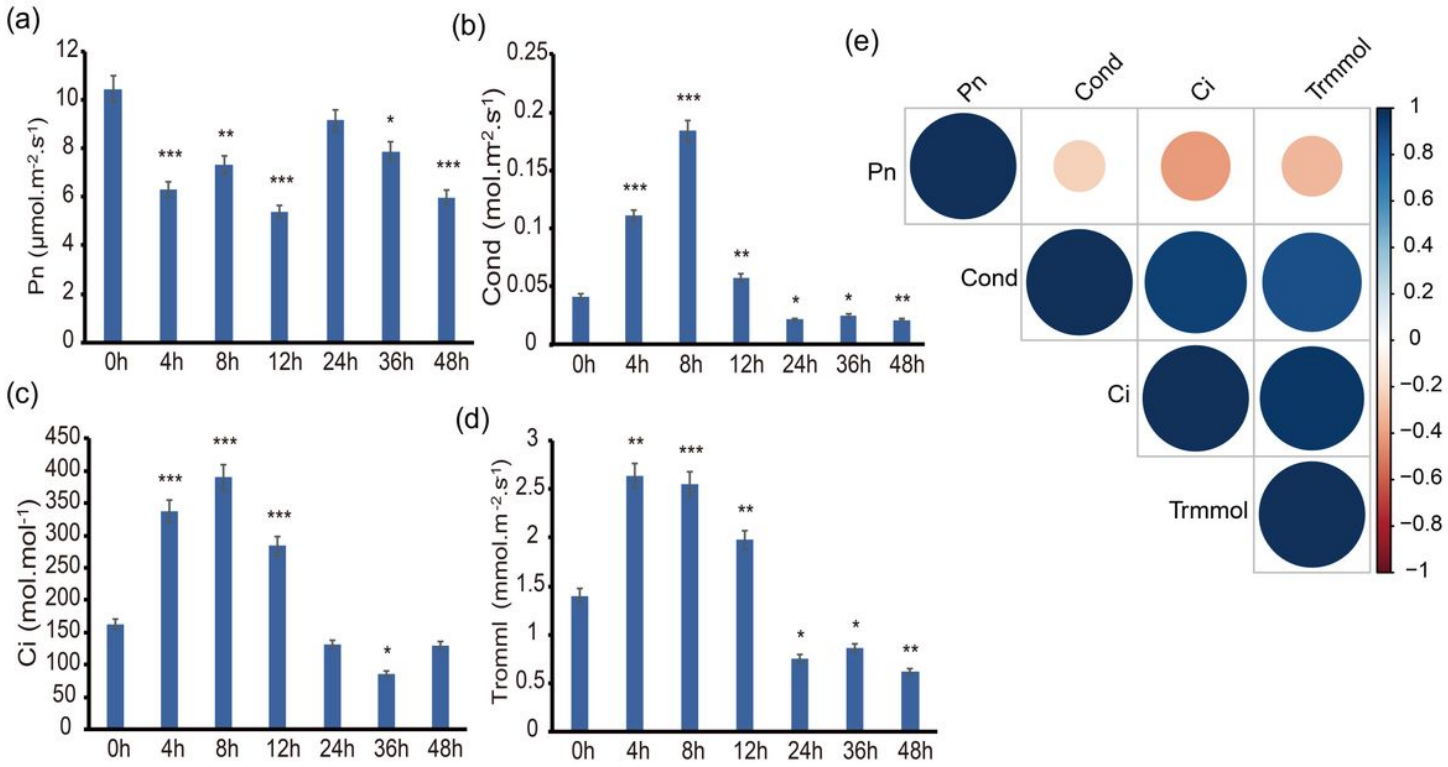

Figure 1

Photosynthetic indices affected by heat stress condition of 0, 4, 8, 12, 24, 36, 48 h. (a) Photosynthesis rate. (b) Stomatal conductance. (c) Intercellular carbon dioxide concentration and (d) Transpiration rate Error bars indicate standard deviation (SD) of three biological replicates. Asterisks indicate significant differences between 0 h and other time points (***P <0001, **P <001, *P <005). (e) Correlations among the four traits. Red represents high adjacency (positive correlation) and blue represents low adjacency (negative correlation).

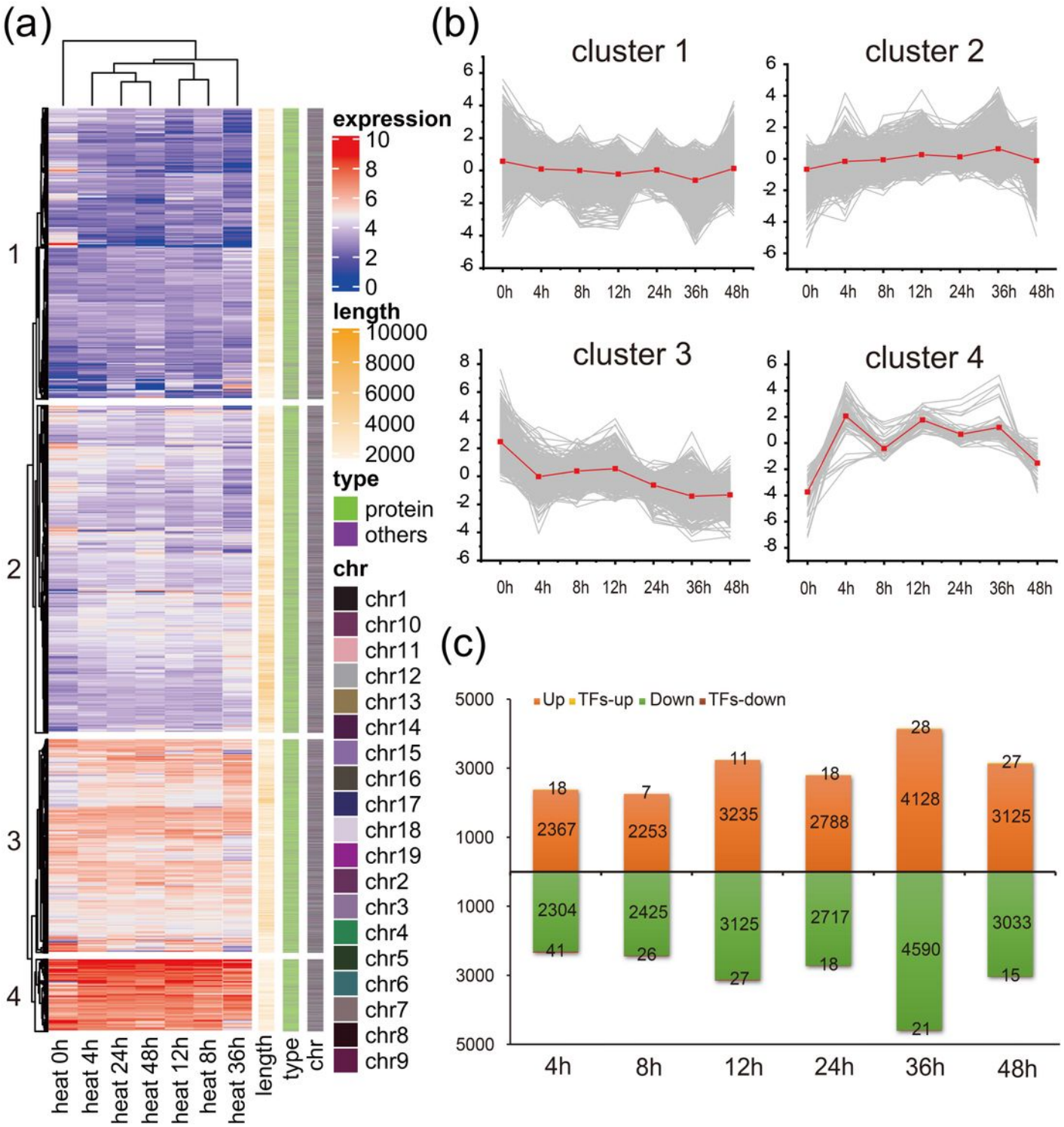

Figure 2

P trichocarpa response patterns of the differentially expressed genes (DEGs) under seven heat stress treatments (0, 4, 8, 12, 24, 36, and 48 h). (a) Genes clustered into four groups based on their response patterns (genes are listed in Additional file 1). (b) Response patterns of the four DEGs groups. (c) The number of upregulated (upper bars) and downregulated (lower bars) genes at each heat treatment time

compared with the control group (0 h). Numbers of the up- or down-regulated transcription factors (TFs) at each heat treatment time is given.

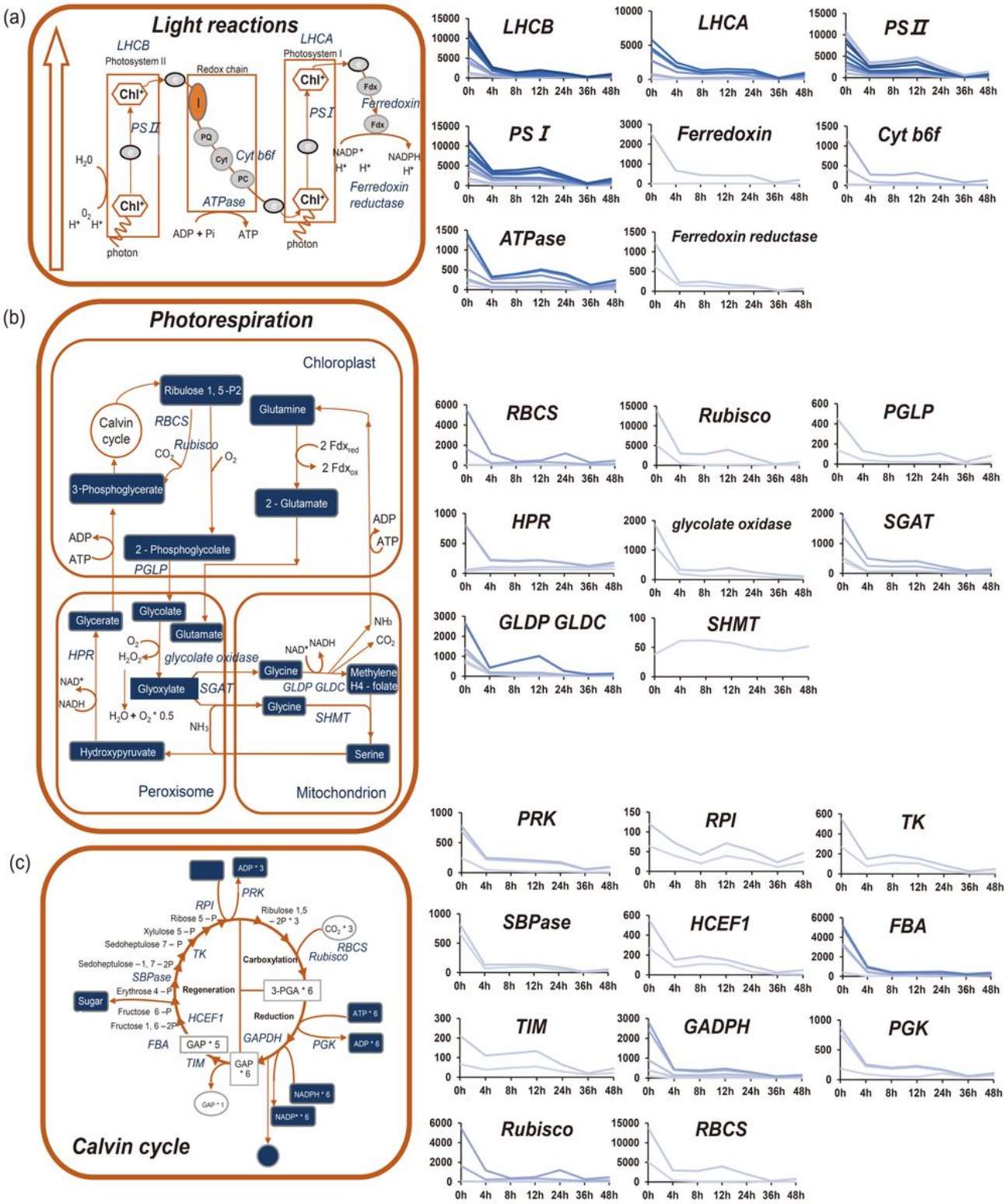

Figure 3

The photosynthesis pathway under heat stress. The expression levels of genes are exhibited on the right. (a)-(c) Showing three pathways of photosynthesis, light reaction, photorespiration and Calvin cycle.

Labeled numbers on represent different types of gene family with each family's expression is shown on the right panel.

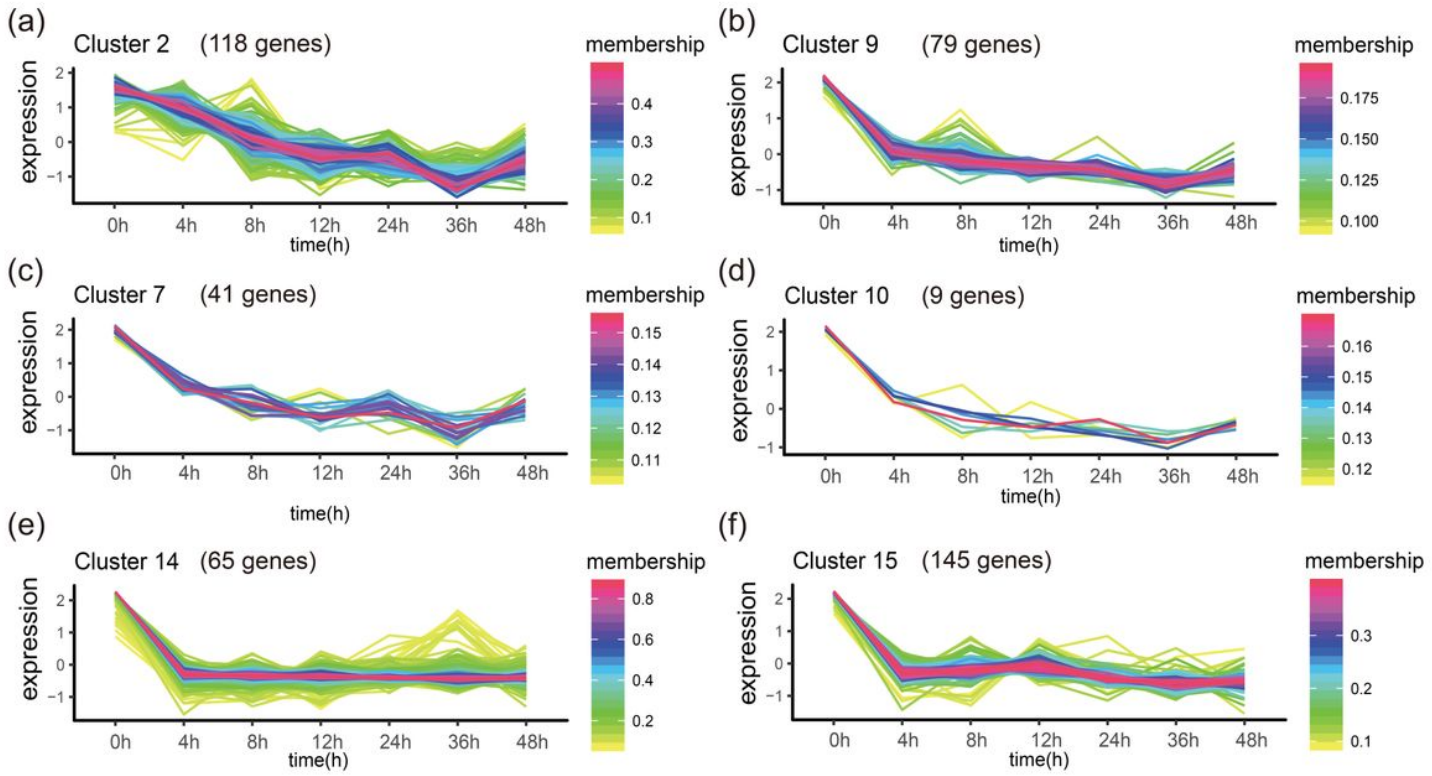

Figure 4

Six out of 18 patterns of highly photosynthesis related genes under heat stress of P. trichocarpa. The response patterns included seven time points: 0, 4, 8, 12, 24, 36, and 48 h under heat stress. Bars on the right represent the abundance of DEGs. The patterns of all clusters were shown in Supplementary Figure 3.

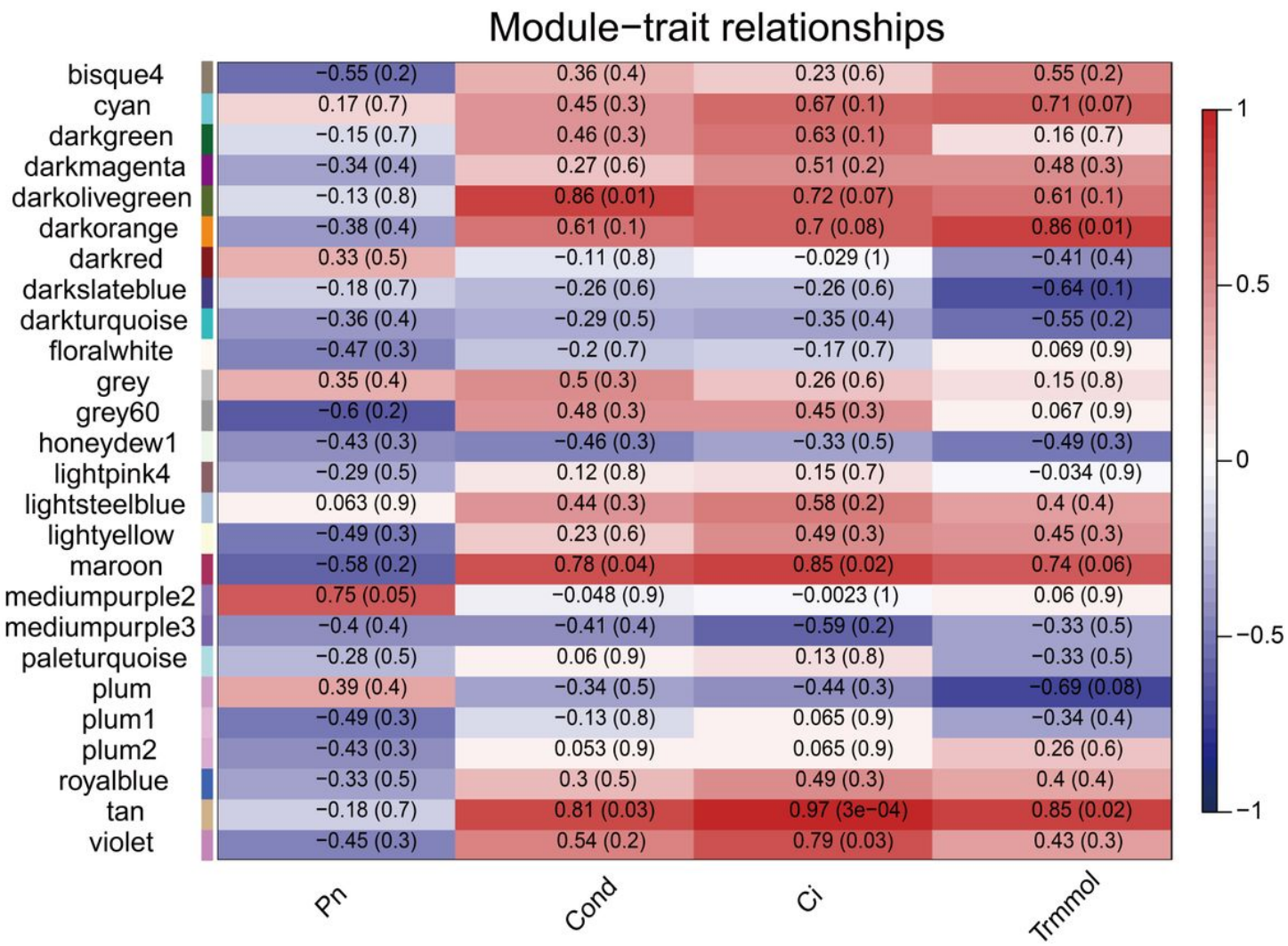

Figure 5

Relationships of consensus module eigengenes and different stages of hepatocellular carcinoma (HCC). Each row in the table corresponds to a consensus module, and each column to a stage. The module name is shown on the left side of each cell. Numbers in the table report the correlations of the corresponding module eigengenes and stage, with the P values printed next to the correlation value in parentheses. The table is color-coded where red and blue represent positive and negative correlations, respectively. Intensity and direction of correlations are indicated by the heatmap on the table's right side.

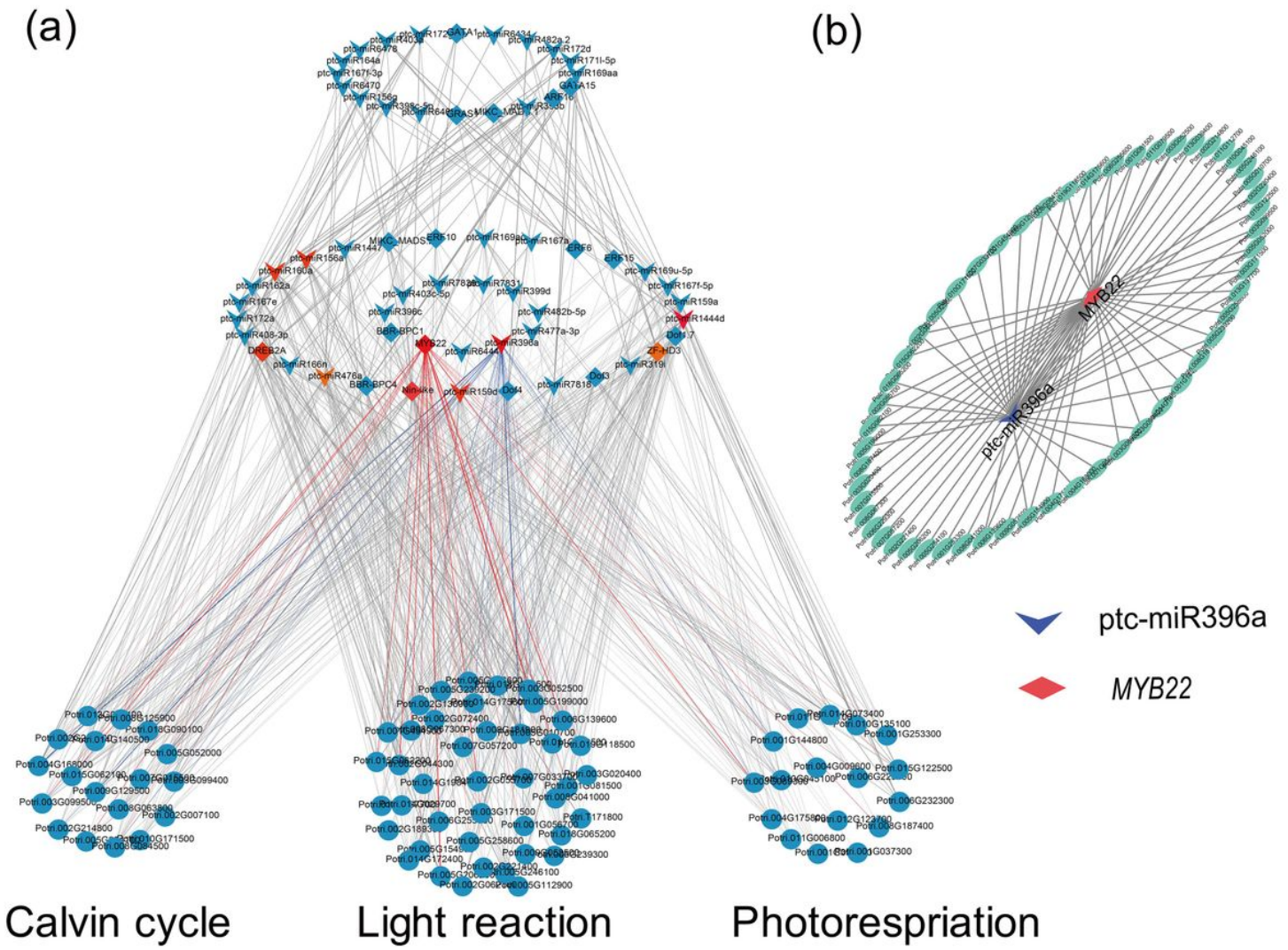

Figure 6

(a) A three-layer genetic regulatory network (GRN) indicating the control of 42 light reaction, 18 Calvin cycle, and 17 photorespiration genes. MiRNAs were shown as a shape of ‘V’, TFs as squares, and genes as circles. On the bottom layer, 42 genes are shown as direct targets of most TFs and miRNAs in layer 2. Some genes in photorespiration are included in the GRN also because of proposed interaction with TFs and miRNAs in layer 2. The thickness of the connecting lines reflects the calculated relative strength of the proposed interaction. The remainder of layer 2 is composed of TFs and target miRNAs selected by the GGM algorithm based on putative interactions with genes in the bottom layer. Similarly, layer 3 (top layer) represents TFs and miRNAs derived by GGM based on interactions with layer 2 as described in Materials and Methods. (b) Gene regulatory network based on the targets and corresponding regulated downstream genes. The blue, red, and green represent the miR396a, MYB22, and green represents the downstream regulated genes, respectively.

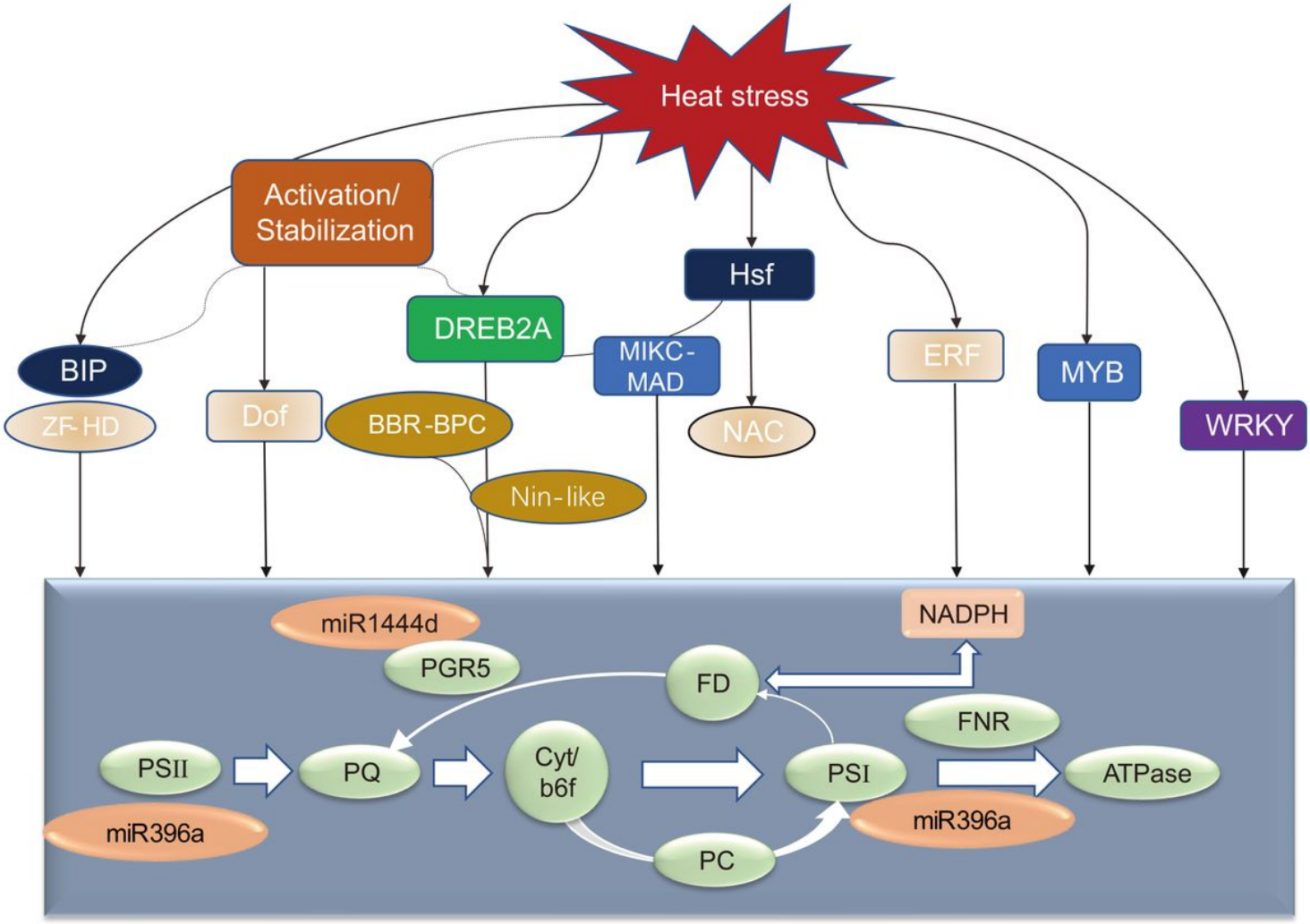

Figure 7

Schematic model of genes participating in the photosynthetic pathway under heat stress. In the present study, the TFs were identified and their detailed information about are provided in Additional file 5.

Supplementary Files

This is a list of supplementary files associated with this preprint. Click to download.

- Additionalfile5.xlsx
- Additionalfile9.xlsx
- Additionalfile7.xlsx
- SupportingdataSupplementaryFigure18AdditionalFile19.doc
- Additionalfile2.xlsx
- Additionalfile3.xlsx
- Additionalfile4.xlsx